Available online at www.sciencedirect.com
SCIENCE DIRECT
Journal of Colloid and Interface Science 289 (2005) 94–103
JOURNAL OF Colloid and Interface Science
www.elsevier.com/locate/jcis

Photophoresis of an aerosol sphere normal to a plane wall

Huan J. Keh *, Fu C. Hsu

Department of Chemical Engineering, National Taiwan University, Taipei 106-17, Taiwan, Republic of China

Received 22 November 2004; accepted 21 March 2005

Available online 27 April 2005

Abstract

A combined analytical–numerical study is presented for the quasisteady photophoretic motion of a spherical aerosol particle of arbitrary thermal conductivity and surface properties exposed to a radiative flux perpendicular to a large plane wall. The Knudsen number is assumed to be so small that the fluid flow is described by a continuum model with a temperature jump, a thermal slip, and a frictional slip at the surface of the radiation-absorbing particle. In the limit of small Peclet and Reynolds numbers, the appropriate equations of conservation of energy and momentum for the system are solved using a boundary collocation method and numerical results for the photophoretic velocity of the particle are obtained for various cases. The presence of the neighboring wall causes two basic effects on the particle velocity: first, the local temperature gradient on the particle surface is enhanced or reduced by the wall, thereby speeding up or slowing down the particle; second, the wall increases viscous retardation of the moving particle. The net effect of the wall can decrease or increase the particle velocity, depending upon the relative conductivity and surface properties of the particle as well as the relative particle–wall separation distance. In general, the boundary effect of a plane wall on the photophoresis of an aerosol particle can be quite significant in some situations. In most aerosol systems, the boundary effect on photophoresis is weaker than that on the motion driven by a gravitational field.

Keywords: Photophoresis; Aerosol sphere; Thin Knudsen layer; Boundary effect

1. Introduction

Small particles, when suspended in a gaseous medium and exposed to an intense light beam, will migrate parallel to the direction of the light. This phenomenon is a result of the uneven heating of the light-absorbing particle (and therefore of its adjacent gas molecules) and is known as photophoresis [1]. The photophoretic (or thermophoretic) effect can be explained in part by appealing to the kinetic theory of gases [2,3]. The higher energy molecules in the hot region of the gas impinge on the particle with greater momenta than molecules coming from the cold region, thereby leading to the migration of the particle in a direction opposite to the surface temperature gradient. Thus, the photophoretic force on an aerosol particle can be directed either toward (negative photophoresis) or away from (positive photophoresis) the light source, depending upon the optical characteristics of the particle. If the particle is opaque and the incident light energy is absorbed and dissipated directly at the front surface of the particle, positive photophoresis occurs. Conversely, if the light beam is partially transmitted and focused on the rear side of the particle, negative photophoresis may appear.

Photophoresis has been observed for many particulate materials in the diameter range between 10^{-8} and 10^{-3} m, and at pressures from above 1 atm down to below 1 Torr, under illumination intensities comparable with those of sunlight [4]. Therefore, the results of photophoretic investigations are of interest to a wide variety of fields including cloud physics, aerosol science, and environmental engineering. For example, measurements of the photophoretic force or the reversal point from positive to negative photophoresis with the elaboration of photophoretic spectroscopy can be used to determine the physical properties, such as the complex refractive index, and the chemical composition of aerosol particles [5]. The photophoretic phenomena of aerosol particles

* Corresponding author.
E-mail address: huan@ntu.edu.tw (H.J. Keh).

0021-9797/$ – see front matter
doi:10.1016/j.jcis.2005.03.047

subjected to coherent light beams have been applied to the development of laser atmospheric monitoring methods [6]. It was found that, due to the effect of both positive and negative photophoresis, some stratospheric aerosol particles may be caused to rise against gravity, whereas others are induced to fall considerably more rapidly than they would under gravity alone [7]. Considering that radiative heat transfer can account for around 95% of the total heat flux in pulverized-coal furnaces, the driving force for photophoresis of small particles in combustion environments can be significantly greater than that for thermophoresis [8].

When the Knudsen number (l/a, where a is the radius of the particle and l is the mean free path of the surrounding gas molecules), Reynolds number, and Peclet number are small, the photophoretic velocity of an aerosol sphere illuminated by an intense light beam can be expressed as [8,9]

$$U_0 = -\frac{2JC_s\eta I}{3(1+2C_m l/a)(2k+k_p+2k_p C_t l/a)\rho_f T_0}. \quad (1)$$

In the above equation, I is the intensity of the incident light (incoming illumination energy flux); ρ_f, η, and k are the density, viscosity, and thermal conductivity, respectively, of the gas; k_p is the thermal conductivity of the particle; T_0 is the absolute temperature of the bulk gas; J is the so-called photophoretic asymmetry factor [10], which can be either positive (negative photophoresis) or negative (positive photophoresis); C_s, C_t, and C_m are dimensionless coefficients accounting for the thermal slip, temperature jump, and frictional slip phenomena, respectively, at the particle surface and must be determined experimentally for each gas–solid system. A set of reasonable kinetic-theory values for complete thermal and momentum accommodation appear to be $C_s = 1.17$, $C_t = 2.18$, and $C_m = 1.14$ [11]. Recently, kinetic-theory values of these slip coefficients have been obtained accurately under various conditions [12,13]. Note that the photophoretic velocity given by Eq. (1) is proportional to the fluid viscosity due to the existence of the thermal slip velocity at the particle surface.

In many applications of photophoresis, aerosol particles are not isolated and will move in the presence of neighboring particles and/or boundaries. For example, the mechanism and rate of deposition of photophoretic particles on various surfaces are of practical interest. It is of some importance, therefore, to examine the behavior of a particle under photophoretic forces as it is in the proximity of rigid boundaries. Recently, the quasisteady photophoresis of an aerosol sphere located at the center of a spherical cavity has been investigated and an analytical expression for the wall-corrected particle velocity was derived in a closed form [14]. In this work we present an analysis of the photophoretic motion of an aerosol sphere perpendicular to an infinite plane wall. The quasisteady equations of conservation applicable to the system are solved by a combined analytical–numerical method using the boundary collocation technique. Results for the wall-corrected particle velocity are obtained with good convergence for various cases.

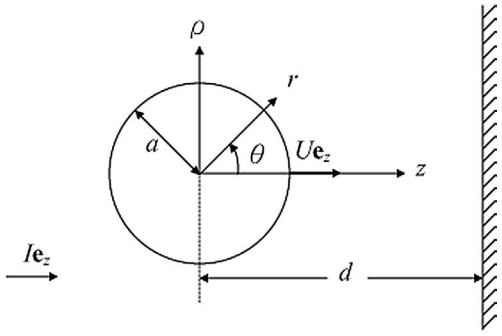

Fig. 1. Geometrical sketch for the photophoretic motion of a spherical particle perpendicular to a plane wall.

2. Analysis

We consider the quasisteady photophoretic motion of a spherical particle of radius a with arbitrary thermal conductivity and surface properties in a gaseous medium transparent to radiation in the direction normal to an infinite plane wall located at a distance d from the particle center, as illustrated in Fig. 1. Here, (ρ,ϕ,z) and (r,θ,ϕ) denote the circular cylindrical and spherical coordinate systems, respectively, and both origins of coordinates are set at the center of the particle. The incident light is imposed to the particle in the z direction (perpendicular to the wall) with intensity I and the photophoretic velocity of the particle is $U\mathbf{e}_z$, where $\mathbf{e}_z$ is the unit vector in the positive z direction. Both of the bulk gas and the plane wall are kept at a constant temperature T_0. The Knudsen numbers l/a and $l/(d-a)$ are assumed to be so small that the fluid flow is in the continuum regime and the Knudsen layer adjacent to the surface of the particle is relatively thin. The fluid is allowed to slip, both thermally and frictionally, and the temperature jump may occur at the particle surface. Our objective is to determine the correction to Eq. (1) for the photophoretic particle due to the presence of the plane wall.

To determine the photophoretic velocity of the particle, it is necessary to ascertain the temperature and fluid velocity distributions.

2.1. Temperature distribution

The Peclet number of this axisymmetric problem is assumed to be small. Hence, the equation of energy governing the temperature distribution $T(r,\theta)$ for the fluid of constant thermal conductivity k is the Laplace equation,

$$\nabla^2 T = 0. \quad (2)$$

The temperature distribution $T_p(r,\theta)$ inside the radiation-absorbing particle is described by

$$\nabla^2 T_p = -\frac{1}{k_p} Q(r,\theta), \quad (3)$$

where k_p is the thermal conductivity of the particle and $Q(r,\theta)$ is the volumetric thermal energy generation rate re-

sulting from local radiation absorption. For a plane monochromatic wave, the source function $Q(r,\theta)$ is related to the electric field $\mathbf{E}(r,\theta)$ inside the particle according to the Lorenz–Mie theory [7,15],

$$Q(r,\theta) = \frac{4\pi\upsilon\kappa I}{\lambda}\frac{|\mathbf{E}(r,\theta)|^2}{|\mathbf{E}_0|^2} = \frac{4\pi\upsilon\kappa I}{\lambda}B(\zeta,\theta). \tag{4}$$

Here, υ and κ are the real and imaginary parts of the complex refractive index $\overline{N}$ ($\overline{N} = \upsilon + i\kappa$) of the particle, $\mathbf{E}_0$ is the incident electric field strength, λ is the wavelength of the incident radiation, $B(\zeta,\theta)$ is the dimensionless electric field distribution function, and $\zeta = r/a$ is the dimensionless radial spherical coordinate.

The boundary conditions at the particle surface ($r = a$) require that the normal heat fluxes be continuous and a temperature jump that is proportional to the normal temperature gradient [3] occur. Also, the fluid temperature at the plane wall or far removed from the particle approaches the bulk-gas temperature T_0, which is a constant. Thus,

$$r = a: \qquad k\frac{\partial T}{\partial r} = k_{\mathrm{p}}\frac{\partial T_{\mathrm{p}}}{\partial r}, \tag{5a}$$

$$T - T_{\mathrm{p}} = C_{\mathrm{t}} l\frac{\partial T}{\partial r}, \tag{5b}$$

$$z = d: \qquad T = T_0, \tag{6}$$

$$r \to \infty \text{ and } z \leqslant d: \quad T = T_0, \tag{7}$$

where C_{t} is the temperature jump coefficient on the particle surface. In Eq. (5a), the flux due to radiative heat transfer, which was taken into account by Akhtaruzzaman and Lin [16] in studying the photophoresis of a spherical particle in the free molecule regime (in a rarefied gas with large Knudsen number), is neglected on the assumption that the surface temperature of the particle is not very high. The Knudsen layer adjacent to the isothermal plane wall is neglected for the case of small Knudsen number.

Since the governing equations and boundary conditions are linear, one can write the temperature distribution T as the superposition

$$T = T_0 + T_{\mathrm{w}} + T_{\mathrm{s}}. \tag{8}$$

Here, T_{w} is a Fourier–Bessel integral solution of Laplace's equation in cylindrical coordinates that represents the disturbance produced by the plane wall and is given by

$$T_{\mathrm{w}} = \int_0^\infty \omega R(\omega) J_0(\omega\rho) e^{\omega z}\,\mathrm{d}\omega, \tag{9}$$

where J_0 is the Bessel function of the first kind of order zero and $R(\omega)$ is an unknown function of ω. The last term on the right-hand side of Eq. (8), T_{s}, is the solution of Laplace's equation in spherical coordinates, representing the disturbance generated by the particle, and is given by an infinite series in harmonics,

$$T_{\mathrm{s}} = \frac{aI}{k}\sum_{n=0}^{\infty} T_n \zeta^{-(n+1)} P_n(\cos\theta), \tag{10}$$

where P_n is the Legendre polynomial of order n and T_n are the unknown coefficients to be determined. Note that a solution for T in the form given by Eqs. (8)–(10) immediately satisfies boundary condition (7).

Since the temperature is finite for any position in the interior of the particle, the solution to Eq. (3) can be written as [8,9]

$$T_{\mathrm{p}} = T_0 + \frac{aI}{k_{\mathrm{p}}}\sum_{n=0}^{\infty}\big[H_n\zeta^n + S_n(\zeta)\big]P_n(\cos\theta), \tag{11}$$

where

$$S_n(\zeta) = \frac{2\pi\upsilon\kappa a}{\lambda} \times\left[\zeta^n\int_\zeta^1 t^{-n+1}\int_0^\pi B(t,\theta)P_n(\cos\theta)\sin\theta\,\mathrm{d}\theta\,\mathrm{d}t + \zeta^{-n-1}\int_0^\zeta t^{n+2}\int_0^\pi B(t,\theta)P_n(\cos\theta)\sin\theta\,\mathrm{d}\theta\,\mathrm{d}t\right], \tag{12}$$

and H_n are unknown coefficients.

A brief conceptual description of the solution procedure to determine $R(\omega)$ and T_n is given below to help the readers follow the mathematical development. At first, boundary condition (6) is exactly satisfied on the plane wall using a Hankel transform. This permits the unknown function $R(\omega)$ to be determined in terms of the coefficients T_n. Then, the boundary conditions on the particle surface given by Eqs. (5) can be satisfied by making use of the collocation method and the solution of the collocation matrix provides numerical values for the coefficients T_n.

Substitution of the solution T given by Eqs. (8)–(10) into the boundary condition (6) and application of the Hankel transform on the variable ρ lead to a solution for $R(\omega)$ in terms of the unknown coefficients T_n. After the substitution of this solution into Eq. (9), the resulting temperature field T is given by

$$T = T_0 + \frac{aI}{k}\sum_{n=0}^{\infty} T_n a^{n+1}\big[B_n''(\rho,z) - B_n''(\rho,2d-z)\big], \tag{13}$$

where the function $B_n''(\rho,z)$ is defined by Eq. (A.5b) in Appendix A. Equation (13) provides an exact solution for the temperature distribution in the fluid phase and the unknown coefficients T_n must be determined from the remaining boundary conditions on the particle surface.

Utilizing the relation

$$\frac{\partial}{\partial r} = \sin\theta\frac{\partial}{\partial\rho} + \cos\theta\frac{\partial}{\partial z}, \tag{14}$$

one can apply Eqs. (5) to Eqs. (11) and (13) to yield

$$\sum_{n=0}^{\infty}\big\{T_n a^{n+1}\alpha_n'(\rho,z) - \big[nH_n + S_n'(\zeta)\big]P_n(\cos\theta)\big\} = 0, \tag{15a}$$

$$\sum_{n=0}^{\infty}\{T_n k^* a^{n+1}\big[B_n''(\rho,z)-B_n''(\rho,2d-z)-C_t^*\alpha_n'(\rho,z)\big] - \big[H_n+S_n(\zeta)\big]P_n(\cos\theta)\}=0 \tag{15b}$$

at $\zeta=1$. Here, the function $\alpha_n'(\rho,z)$ is defined by Eq. (A.1a), $k^*=k_p/k$, $C_t^*=C_t l/a$, and the prime on $S_n(\zeta)$ means differentiation with respect to ζ. Note that the dimensionless parameter $k^*C_t^*$ denotes the relative resistance caused by the temperature jump at the particle surface with respect to heat conduction inside the particle.

To satisfy the conditions in Eqs. (15) exactly along the entire surface of the particle would require the solution of the infinite series of unknown coefficients T_n. However, the collocation technique [17–19] enforces the boundary conditions at a finite number of discrete points on the semicircular generating arc of the particle and truncates the infinite series in Eqs. (11) and (13) into finite ones. If the spherical boundary is approximated by satisfying conditions in Eqs. (5) at N discrete points (values of θ) on its generating arc, then the infinite series in Eqs. (11) and (13) are truncated after N terms, resulting in a system of $2N$ simultaneous linear algebraic equations in the truncated form of Eqs. (15). This matrix equation can be solved to yield the $2N$ unknown coefficients T_n and H_n required in the truncated form of Eqs. (11) and (13) for the temperature distribution. The accuracy of the truncation technique can be improved to any degree by taking a sufficiently large value of N. Naturally, as $N\to\infty$ the truncation error vanishes.

2.2. Fluid velocity distribution

Having obtained the solution for the temperature distribution on the particle surface which drives the migration, we can now proceed to find the flow field. The fluid surrounding the particle is assumed to be incompressible and Newtonian. Due to the low Reynolds number, the fluid motion caused by the photophoretic migration of the particle is governed by the quasisteady fourth-order differential equation for axisymmetric creeping flows,

$$E^4\Psi=E^2\big(E^2\Psi\big)=0, \tag{16}$$

where the Stokes stream function Ψ is related to the velocity components in cylindrical coordinates by

$$v_\rho=\frac{1}{\rho}\frac{\partial\Psi}{\partial z}, \tag{17a}$$

$$v_z=-\frac{1}{\rho}\frac{\partial\Psi}{\partial\rho}, \tag{17b}$$

and the operator E^2 has the form

$$E^2=\rho\frac{\partial}{\partial\rho}\left(\frac{1}{\rho}\frac{\partial}{\partial\rho}\right)+\frac{\partial^2}{\partial z^2}. \tag{18}$$

Owing to the thermal and frictional slip velocities along the particle surface, the boundary conditions for the fluid velocity at the particle surface are [20]

$$r=a:\quad v_r=U\cos\theta, \tag{19a}$$

$$v_\theta=-U\sin\theta+\frac{C_m l}{\eta}\tau_{r\theta}+\frac{C_s\eta}{\rho_f T_0 r}\frac{\partial T}{\partial\theta}. \tag{19b}$$

Here, v_r and v_θ are the velocity components in spherical coordinates, C_m and C_s are the frictional and thermal slip coefficients, respectively, on the surface of the particle, $\tau_{r\theta}$ is the shear stress for the fluid flow,

$$\tau_{r\theta}=\eta\left[r\frac{\partial}{\partial r}\left(\frac{v_\theta}{r}\right)+\frac{1}{r}\frac{\partial v_r}{\partial\theta}\right], \tag{20}$$

and U is the photophoretic velocity of the particle, to be determined. The derivative $\partial T/\partial\theta$ at the particle surface can be evaluated from the temperature distribution given by Eq. (13) with coefficients T_n determined from Eqs. (15). The thermal slip velocity expressed by the last term in Eq. (19b) is proportional to the fluid viscosity due to the fact that the tangential stress of the fluid caused by the temperature gradient along the particle surface is proportional to the product of the temperature gradient (or momentum gradient) and the kinematic viscosity of the fluid, and the validity of this expression is based on the assumption that the fluid temperature is only slightly nonuniform on the length scale of the particle radius. Generally speaking, the slip condition becomes increasingly more important for small particles. At the isothermal plane wall and far away from the particle, the boundary conditions for the fluid velocity are

$$z=d:\qquad v_\rho=v_z=0, \tag{21}$$

$$r\to\infty \text{ and } z\leqslant d:\quad v_\rho=v_z=0. \tag{22}$$

The effect of gas slip at the plane wall is negligible since the plane is isothermal and the Knudsen number is small.

The stream function for the fluid flow is linearly composed of two parts:

$$\Psi=\Psi_w+\Psi_s. \tag{23}$$

Here Ψ_w is a solution of Eq. (16) in cylindrical coordinates that represents the disturbance produced by the plane wall and is given by a Fourier–Bessel integral,

$$\Psi_w=\int_0^\infty \rho J_1(\omega\rho)\big[X(\omega)+zY(\omega)\big]e^{\omega z}\,d\omega, \tag{24}$$

where J_1 is the Bessel function of the first kind of order one, and $X(\omega)$ and $Y(\omega)$ are unknown functions of ω. The second part of Ψ, denoted by Ψ_s, is a solution of Eq. (16) in spherical coordinates representing the disturbance generated by the particle and is given by

$$\Psi_s=Ua^2\sum_{n=2}^{\infty}\big(B_n\zeta^{-n+1}+D_n\zeta^{-n+3}\big)G_n^{-1/2}(\cos\theta), \tag{25}$$

where $G_n^{-1/2}$ is the Gegenbauer polynomial of the first kind of order n and degree $-1/2$, and B_n and D_n are unknown constants. Note that boundary condition (22) is immediately satisfied by a solution of the form given by Eqs. (23)–(25).

As was the case with the solution for the temperature distribution, the determination of $X(\omega)$, $Y(\omega)$, B_n, and D_n

will be undertaken by a two-step procedure. First, boundary condition (21) is exactly satisfied on the plane wall by a Hankel transform; then, the boundary conditions given by Eq. (19) are satisfied numerically at collocation points on the particle surface. Application of boundary condition (21) to Eqs. (23)–(25) using Eq. (17) leads to a solution for $X(\omega)$ and $Y(\omega)$ in terms of the unknown coefficients B_n and D_n. This solution is substituted back into Eq. (24), leading to a new expression for the stream function. The result for the velocity components is

$$v_\rho = U\sum_{n=2}^{\infty}\left[B_n a^{n+1}\beta_n'(\rho,z) + D_n a^{n-1}\delta_n'(\rho,z)\right], \tag{26a}$$

$$v_z = U\sum_{n=2}^{\infty}\left[B_n a^{n+1}\beta_n''(\rho,z) + D_n a^{n-1}\delta_n''(\rho,z)\right], \tag{26b}$$

where the functions β_n', δ_n', β_n'', and δ_n'' are defined by Eqs. (A.2) and (A.3).

The only boundary conditions that remain to be satisfied are those on the particle surface. Substituting Eq. (13) into Eq. (19), one obtains

$$v_\rho = \frac{C_{\mathrm{m}}^* a}{\eta}\tau_{r\theta}\cos\theta + \frac{C_{\mathrm{s}}\eta I}{\rho_{\mathrm{f}} T_0 k}\cos\theta\sum_{n=0}^{\infty} T_n a^{n+1}\alpha_n''(\rho,z), \tag{27a}$$

$$v_z = U - \frac{C_{\mathrm{m}}^* a}{\eta}\tau_{r\theta}\sin\theta - \frac{C_{\mathrm{s}}\eta I}{\rho_{\mathrm{f}} T_0 k}\sin\theta\sum_{n=0}^{\infty} T_n a^{n+1}\alpha_n''(\rho,z) \tag{27b}$$

at $r=a$, where $C_{\mathrm{m}}^* = \mathrm{C_m} l/a$ and the definition of $\alpha_n''(\rho,z)$ is given by Eq. (A.1b). Here the first N coefficients T_n have been determined through the procedure given in the previous section. Application of these boundary conditions to Eqs. (26) can be accomplished by utilizing the collocation technique presented for the solution of the temperature field. At the particle surface, boundary conditions in Eq. (27) are applied at M discrete points (values of θ) and the infinite series in Eqs. (26) are truncated after M terms. This generates a set of $2M$ linear algebraic equations for the $2M$ unknown coefficients B_n and D_n. The fluid velocity field is completely solved once these coefficients are determined.

2.3. Velocity of the particle

The drag force exerted by the fluid on the spherical boundary $r=a$ can be determined from [21]

$$F = \eta\pi\int_0^{\pi} r^3\sin^3\theta\,\frac{\partial}{\partial r}\left(\frac{E^2\Psi}{r^2\sin^2\theta}\right)r\,\mathrm{d}\theta. \tag{28}$$

Substitution of Eqs. (23)–(25) into the above integral and application of the orthogonality properties of the Gegenbauer polynomials result in the simple relation

$$F = 4\pi\eta D_2. \tag{29}$$

This shows that only the coefficient D_2 contributes to the drag force on the particle.

Since the photophoretic particle is freely suspended in the fluid, the net force exerted by the fluid on the surface of the particle must vanish. From Eq. (29), we have $D_2 = 0$. The photophoretic velocity U of the particle can be obtained by satisfying this constraint.

The normalized particle velocity U/U_0 will be a function of the parameters k^*, C_{t}^*, C_{m}^*, and a/d, where U_0 is the photophoretic velocity of the particle in the absence of the plane wall and is given by Eq. (1), or

$$U_0 = -\frac{2JC_{\mathrm{s}}\eta I}{3(1+2C_{\mathrm{m}}^*)(2+k^*+2k^*C_{\mathrm{t}}^*)k\rho_{\mathrm{f}}T_0}. \tag{30}$$

Here J is the so-called photophoretic asymmetry factor,

$$J = \frac{6\pi\upsilon\kappa a}{\lambda}\int_0^1\int_0^{\pi} B(\zeta,\theta)\zeta^3\cos\theta\sin\theta\,\mathrm{d}\theta\,\mathrm{d}\zeta, \tag{31}$$

which depends on the complex refractive index ($\overline{N} = \upsilon + i\kappa$) and the normalized size ($2\pi a/\lambda$) of the particle. The asymmetry factor represents a weighted integration of the heat source function over the particle volume and defines the sign and magnitude of the photophoretic force. If $J<0$, the particle moves in the direction of the light beam (positive photophoresis). If $J>0$, the particle moves in the opposite direction (negative photophoresis). Equation (30) shows that the magnitude of U_0 decreases with an increase in k^*, C_{t}^*, or C_{m}^* for a given value of $JC_{\mathrm{s}}\eta I/k\rho_{\mathrm{f}}T_0$.

For a completely opaque spherical particle the heat sources are concentrated on the illuminated part of the particle surface [9,14]; namely,

$$B(\zeta,\theta) = \begin{cases} \dfrac{-\lambda}{2\pi\upsilon\kappa a}\cos\theta\delta(\zeta-1), & \text{for } \frac{\pi}{2}\leqslant\theta\leqslant\pi, \\ 0, & \text{for } 0\leqslant\theta\leqslant\frac{\pi}{2}, \end{cases} \tag{32}$$

where $\delta(\zeta-1)$ is a Dirac delta function which equals infinity if $\zeta=1$ and vanishes otherwise. The substitution of Eq. (32) into Eq. (31) results in $J=-1/2$ knowing that

$$\int_0^1 g(\zeta)\delta(\zeta-1)\,\mathrm{d}\zeta = (1/2)g(1).$$

If the incident light is transmitted and focused on the rear part of the particle surface, Eq. (32) should be modified in reverse with the angle θ and its substitution into Eq. (31) yields $J=1/2$. Thus, the range of the asymmetry factor is $-1/2\leqslant J\leqslant 1/2$. According to Eq. (30), the photophoretic velocity at on illumination of an intensity comparable to the solar constant (1353 $\mathrm{W\,m^{-2}}$) is on the order of 10^{-5} $\mathrm{m\,s^{-1}}$.

By the linearity of the problem, the same value of the normalized photophoretic velocity is predicted for a given combination of k^*, C_{t}^*, C_{m}^*, and a/d whether the particle is approaching the plane wall or receding from it.

Table 1
Normalized photophoretic mobility of a spherical particle moving perpendicular to a plane wall

a/d	U/U_0							
	$C_t^* = 2C_m^* = 0.02$				$C_t^* = 2C_m^* = 0.2$			
	$k^* = 0$	$k^* = 1$	$k^* = 10$	$k^* = 100$	$k^* = 0$	$k^* = 1$	$k^* = 10$	$k^* = 100$
0	1	1	1	1	1	1	1	1
0.1	0.99615	0.99708	0.99875	1.00576	0.99733	0.99917	1.00681	1.07453
0.2	0.98225	0.98630	0.99356	1.02194	0.98677	0.99438	1.02538	1.29750
0.3	0.95589	0.96563	0.98316	1.04860	0.96541	0.98292	1.05400	1.67337
0.4	0.91522	0.93354	0.96709	1.08841	0.93091	0.96258	1.09221	2.21707
0.5	0.85791	0.88816	0.94508	1.14764	0.88062	0.93077	1.14048	2.95811
0.6	0.78017	0.82634	0.91688	1.23912	0.81066	0.88358	1.19956	3.94480
0.7	0.67557	0.74227	0.88209	1.39044	0.71479	0.81404	1.26856	5.24557
0.8	0.53302	0.62437	0.84021	1.67222	0.58226	0.70800	1.33672	6.91926
0.9	0.33199	0.44385	0.78874	2.33781	0.39035	0.52828	1.33283	8.69112
0.95	0.19723	0.30288	0.74658	3.15679	0.25188	0.37173	1.17040	8.67640
0.99	0.05885	0.11546	0.56164	4.21222	0.08011	0.13257	0.55408	4.67247
0.995	0.03570	0.07447	0.43936	3.79905	0.04577	0.07751	0.34294	2.95778
0.999	0.01071	0.02401	0.18049	1.85088	0.01086	0.01884	0.08861	0.78223

3. Results and discussion

The solution for the photophoretic motion of a spherical particle normal to a plane wall, obtained by using the boundary collocation method described in the previous section, is presented in this section. The system of linear algebraic equations to be solved for the coefficients T_n and H_n is constructed from Eq. (15), while that for B_n and D_n is composed of Eqs. (26) and (27).

In specifying the points along the semicircular generating arc of the sphere (with a constant value of ϕ) where the boundary conditions are to be exactly satisfied, the first point that should be chosen is $\theta = \pi/2$, since this point defines the projected area of the particle normal to the direction of motion. In addition, the points $\theta = 0$ and π are also important because they control the gap between the sphere and the plane. However, an examination of the systems of linear algebraic equations given by Eqs. (15) and (27) shows that the matrix equations become singular if these points are used. To overcome this difficulty, these points are replaced by closely adjacent points, i.e., $\theta = \delta$, $\pi/2 - \delta$, $\pi/2 + \delta$, and $\pi - \delta$. Additional points along the boundary are selected as mirror-image pairs about the plane $\theta = \pi/2$ to divide the two quarter-circular arcs of the particle into equal segments. The optimum value of δ in this work is found to be 0.01°, to which the numerical results of the particle velocity converge satisfactorily.

For the continuum-with-slippage approach employed in this work, the Knudsen number (l/a) of the system should be smaller than about 0.1. As mentioned in the first section, a set of well-adapted values for the temperature jump and frictional slip coefficients under the condition of complete thermal and momentum accommodations are 2.18 and 1.14, respectively. Consequently, the normalized coefficients C_t^* and C_m^* must be restricted to be less than unity. For convenience we will use the ratio $C_t^*/C_m^* = 2$ (rounded from $2.18/1.14 = 1.91$) throughout this section, without loss of reality or generality. On the other hand, although the silica aerogel can have a low thermal conductivity comparable to that of nonmetallic gases [22], the thermal conductivity of an aerosol particle is typically much higher than that of the surrounding gas. Thus, the value of the relative conductivity k^* will exceed unity under most practical circumstances.

The collocation solutions for the wall-corrected reduced photophoretic mobility of an opaque spherical particle with the heat source distribution function given by Eq. (32) moving perpendicular to a plane wall for various values of the parameters C_m^* $(= C_t^*/2)$, k^*, and a/d are presented in Table 1 and depicted in Figs. 2–4. The cases of $k^* < 1$, which are not likely to exist in practice, are considered here for the sake of numerical comparison. All of the results obtained un-

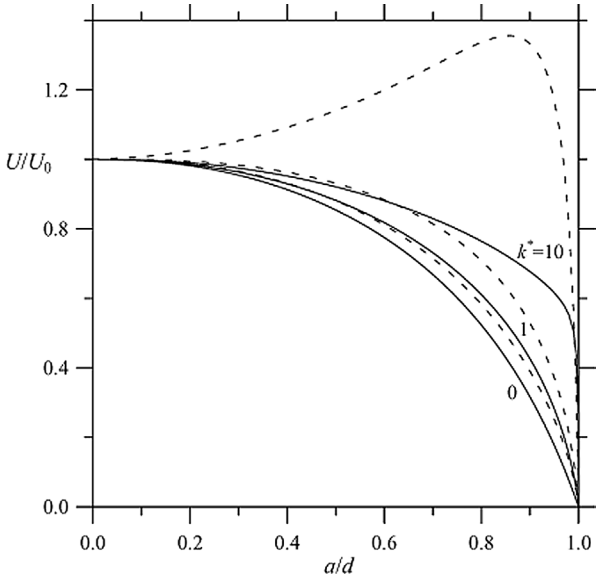

Fig. 2. Plots of the normalized velocity of a spherical particle undergoing photophoresis perpendicular to a plane wall versus the separation parameter a/d for various values of k^*. The solid curves represent the case of $C_t^* = 2C_m^* = 0$, and the dashed curves denote the case of $C_t^* = 2C_m^* = 0.2$.

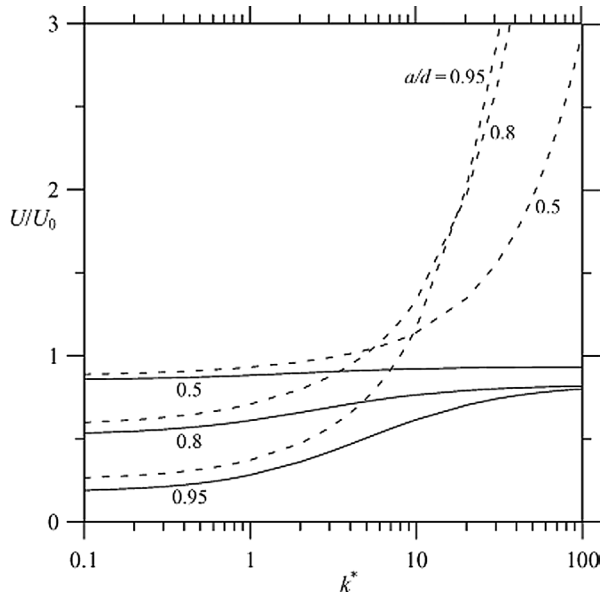

Fig. 3. Plots of the normalized velocity of a spherical particle undergoing photophoresis perpendicular to a plane wall versus the relative thermal conductivity of the particle for various values of the separation parameter a/d. The solid curves represent the case of $C_t^* = 2C_m^* = 0$, and the dashed curves denote the case of $C_t^* = 2C_m^* = 0.2$.

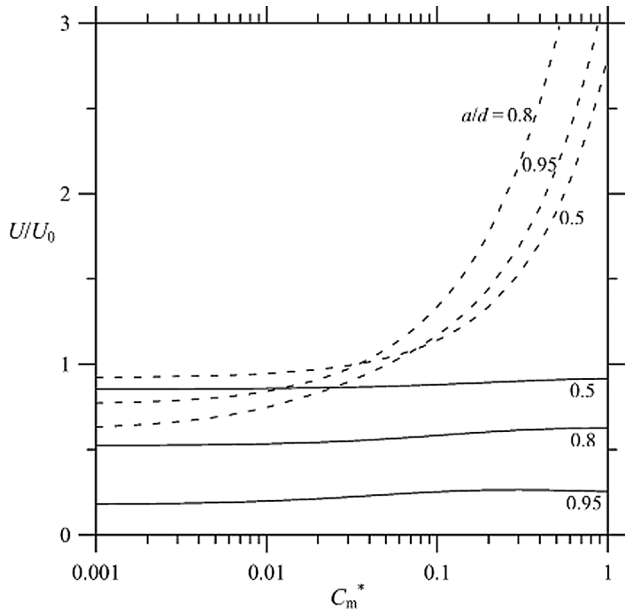

Fig. 4. Plots of the normalized velocity of a spherical particle with $C_t^* = 2C_m^*$ undergoing photophoresis perpendicular to a plane wall versus the normalized frictional slip coefficient for various values of the separation parameter a/d. The solid curves represent the case of $k^* = 0$, and the dashed curves denote the case of $k^* = 10$.

der the collocation scheme converge satisfactorily to at least the significant figures shown in the table. The accuracy and convergence behavior of the truncation technique is principally a function of the relative spacing $(d - a)/a$. For the difficult case with $a/d = 0.999$, the numbers of collocation points $N = 250$ and 250 are sufficiently large to achieve this convergence. As expected, the particle will move with the velocity that would exist in the absence of the wall, given by Eq. (30), as $a/d = 0$. In general, the wall effect on the photophoresis of a particle can be quite significant in practical situations. It should be pointed out that the continuum assumption for the fluid flow in the gap between the particle and the wall might have failed for the table and figures as $a/d > 0.99$ in the case of $C_m^* = 0.01$ and as $a/d > 0.9$ in the case of $C_m^* = 0.1$.

It is found that the normalized photophoretic mobility U/U_0 of the particle increases with an increase in the relative conductivity k^*, keeping the other factors (C_t^*, C_m^*, and a/d) unchanged. The increase in the particle mobility becomes more pronounced as a/d increases. This behavior is expected knowing that the temperature gradients on the particle surface near an isothermal plane wall increase as k^* increases [23]. The value of U/U_0 becomes a sensitive function of k^* if the value of C_m^* or a/d is relatively large. On the other hand, the normalized photophoretic mobility of the particle in general increases with an increase in C_m^* for specified values of k^* and a/d, and U/U_0 is not a sensitive function of C_m^* if the value of C_m^* is small.

Examination of the results shown in Table 1 and Fig. 2 reveals an interesting feature. For the case of a sphere with a relatively small value of k^*, the photophoretic mobility of the particle near the plane wall is a monotonically decreasing function of a/d. For the case of a sphere with a relatively large value of k^*, however, the photophoretic mobility of the particle increases with an increase in a/d when a/d is small, but decreases steadily from a maximum with increasing a/d when a/d is sufficiently large, going to zero in the limit. The locations of the maximum shift to larger values of a/d as the parameter k^* increases or C_m^* decreases. At the maximum point, the particle can move much faster than it would at $a/d = 0$. For example, as $C_t^* = 2C_m^* = 0.2$, $k^* = 100$, and $a/d = 0.9$, the photophoretic velocity can be more than seven times higher than the value with the wall far away from the particle. This interesting feature that U/U_0 may not be a monotonic function of a/d and can even be greater than unity is understandable because the wall effect of hydrodynamic (viscous) resistance on the particle is in competition with the wall effect of thermal enhancement when the particle with a relatively large value of k^* is undergoing photophoretic motion perpendicular to an isothermal plate. It is understood that the value of $l/(d - a)$ may be greater than unity for the case of $a/d \to 1$ (as $C_t^* = 2C_m^* = 0.2$ or 0.02), where the continuum model for the fluid is not likely to be valid in practice. This limiting case is considered here for the sake of numerical comparison. Since the magnitude of U_0 can be quite small at large values of k^* (to which the particle surface temperature is almost uniform), the strong thermal enhancement on the particle velocity can make the value of U/U_0 much greater than unity. This unexpected behavior of wall enhancement on the particle migration also occurs in the case of thermophoresis of an aerosol sphere

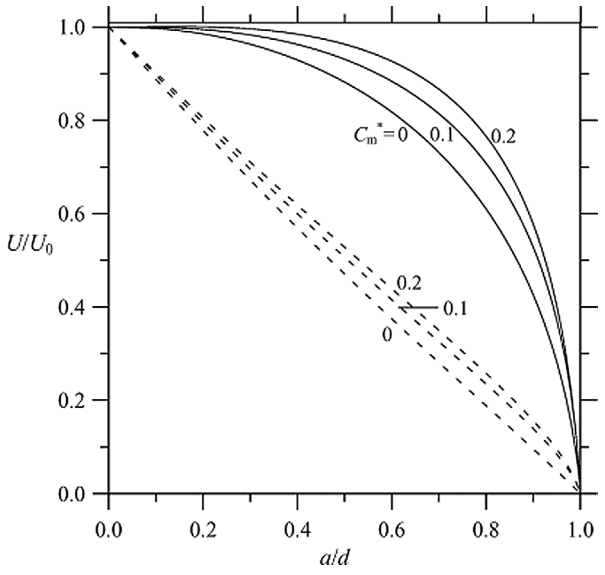

Fig. 5. Plots of the normalized photophoretic mobility (solid curves, with $C_t^* = 2C_m^*$ and $k^* = 1$) and sedimenting mobility (dashed curves) of a spherical particle migrating perpendicular to a plane wall versus the separation parameter a/d for different values of C_m^*.

with a relatively large value of k^* normal to an isothermal plane wall [24].

For the creeping motion of a spherical aerosol particle with a frictional (but isothermal) slip surface on which a constant body force $F\mathbf{e}_z$ (e.g., a gravitational field) is exerted perpendicular to an infinite plane wall, exact results of the particle velocity have been obtained by using spherical bipolar coordinates [25]. A comparison of the boundary effects on the motion of an aerosol sphere under gravity (in which $U_0 = (F/6\pi\eta a)(1 + 3C_m^*)/(1 + 2C_m^*)$) and on the photophoresis of the particle (with $k^* = 1$, so that the effect of heat conduction will not be important) is given in Fig. 5. Similar to the case of photophoresis, the wall effect on the particle motion in a gravitational field is stronger when the value of C_m^* becomes smaller. Evidently, the wall effect on a photophoretic particle in general is much weaker than that on a sedimenting particle.

4. Concluding remarks

In this work, the quasisteady photophoresis of a spherical particle in a gaseous medium normal to a plane wall has been analyzed by using the boundary collocation method. On the basis of the assumption of small Knudsen, Peclet, and Reynolds numbers, the temperature and fluid flow fields for this axisymmetric motion are solved and the wall-corrected particle velocity is obtained. This photophoretic velocity relative to its undisturbed value increases monotonically with an increase in the relative thermal conductivity k^* of the particle. When the value of k^* is sufficiently large, the photophoretic mobility of a particle near a wall may not be a monotonic decreasing function of the separation parameter a/d, and the wall effect can speed up or slow down the particle velocity with respect to its isolated value. This behavior reflects the competition between the weak hydrodynamic retardation exerted by the neighboring wall on the particle migration and the possible relatively strong thermophoretic enhancement due to the thermal interaction between the particle and the wall. The results show that the boundary effect of the plane wall on the photophoretic motion of an aerosol particle can be significant in some situations. In practical aerosol systems, the boundary effect on photophoresis of a particle in general is weaker than that on the particle motion driven by gravity.

In the previous section, we have presented the results of wall-corrected photophoretic mobility calculated from a simplified model for a completely opaque sphere whose heat sources are concentrated on the illuminated part of the particle surface. A calculation according to the Lorenz–Mie theory showed bad applicability of this model even for large strongly absorbing spherical particles [26]. Evidently, if we perform a corresponding calculation for a model transparent sphere with heat sources concentrated completely on the rear half of the particle surface, the same results but with opposite direction (negative photophoresis) will be obtained. If one uses a more consecutive energy-absorbing model than that defined by Eq. (32) for the asymmetry factor J given by Eq. (31) based on the Lorenz–Mie theory, it is expectable that the resulted photophoretic mobility of the sphere will be qualitatively similar to but quantitatively smaller than that obtained from using Eq. (32).

It is worth repeating that our results for the photophoretic velocity are obtained on the basis of a continuum model for the gas phase with slip-flow boundary conditions at the particle surface. For a perfect gas, the kinetic theory predicts that the mean free path of gas molecules is inversely proportional to the pressure [27]. As examples, the mean free path of air molecules at 25 °C is about 67 nm at 1 atm and is about 51 μm at 1 Torr. Therefore, our results obtained with the assumption of small Knudsen number can be used for a broad range of particle sizes around atmospheric pressure but are only applicable to relatively large particles at low pressures.

Acknowledgment

Part of this research was supported by the National Science Council of the Republic of China.

Appendix A. Definitions of some functions in Section 2

For conciseness the definitions of some functions in Section 2 are listed here:

$$\alpha_n'(\rho,z) = \rho\big[A_n(\rho,z) - A_n(\rho,2d-z)\big] - (n+1)z\big[B_{n+1}''(\rho,z) + B_{n+1}''(\rho,2d-z)\big], \tag{A.1a}$$

$$\alpha_n''(\rho,z) = z\big[A_n(\rho,z) - A_n(\rho,2d-z)\big] + (n+1)\rho\big[B_{n+1}''(\rho,z) + B_{n+1}''(\rho,2d-z)\big], \tag{A.1b}$$

$$\beta_n'(\rho,z) = B_n'(\rho,z) - B_n'(\rho,2d-z) + 2(n+1)(d-z)B_{n+1}'(\rho,2d-z), \tag{A.2a}$$

$$\beta_n''(\rho,z) = B_n''(\rho,z) - B_n''(\rho,2d-z) - 2(n+1)(d-z)B_{n+1}''(\rho,2d-z), \tag{A.2b}$$

$$\delta_n'(\rho,z) = D_n'(\rho,z) - D_n'(\rho,2d-z) - (2/n)(n-1)(n-3)(d-z)B_{n-1}'(\rho,2d-z) + 2(2n-3)d(d-z)B_n'(\rho,2d-z), \tag{A.3a}$$

$$\delta_n''(\rho,z) = D_n''(\rho,z) - D_n''(\rho,2d-z) + 2(n-2)(d-z)B_{n-1}''(\rho,2d-z) - 2(2n-3)d(d-z)B_n''(\rho,2d-z), \tag{A.3b}$$

where

$$A_n(\rho,z) = \frac{nz^2-(n+1)\rho^2}{\rho(\rho^2+z^2)^{(n+3)/2}}P_n\left[\frac{z}{(\rho^2+z^2)^{1/2}}\right] - \frac{nz}{\rho(\rho^2+z^2)^{(n+2)/2}}P_{n-1}\left[\frac{z}{(\rho^2+z^2)^{1/2}}\right], \tag{A.4}$$

$$B_n'(\rho,z) = \frac{n+1}{\rho(\rho^2+z^2)^{n/2}}G_{n+1}^{-1/2}\left[\frac{z}{(\rho^2+z^2)^{1/2}}\right], \tag{A.5a}$$

$$B_n''(\rho,z) = \frac{1}{(\rho^2+z^2)^{(n+1)/2}}P_n\left[\frac{z}{(\rho^2+z^2)^{1/2}}\right], \tag{A.5b}$$

$$D_n'(\rho,z) = \frac{n+1}{\rho(\rho^2+z^2)^{(n-2)/2}}G_{n+1}^{-1/2}\left[\frac{z}{(\rho^2+z^2)^{1/2}}\right] - \frac{2z}{\rho(\rho^2+z^2)^{(n-1)/2}}G_n^{-1/2}\left[\frac{z}{(\rho^2+z^2)^{1/2}}\right], \tag{A.6a}$$

$$D_n''(\rho,z) = \frac{2}{(\rho^2+z^2)^{(n-1)/2}}G_n^{-1/2}\left[\frac{z}{(\rho^2+z^2)^{1/2}}\right] + \frac{1}{(\rho^2+z^2)^{(n-1)/2}}P_n\left[\frac{z}{(\rho^2+z^2)^{1/2}}\right]. \tag{A.6b}$$

In the above equations, P_n is the Legendre polynomial of order n and $G_n^{-1/2}$ is the Gegenbauer polynomial of the first kind of order n and degree $-1/2$.

Appendix B. Nomenclature

A_n	functions of ρ and z defined by Eq. (A.4) (m^{-n-2})
a	particle radius (m)
$B(\zeta,\theta)$	dimensionless electric field distribution function defined by Eq. (4)
B_n, D_n	coefficients in Eqs. (25) and (26) for the flow field
B_n', B_n''	functions of ρ and z defined by Eqs. (A.5) (m^{-n-1})
C_m	coefficient accounting for the frictional slip at the particle surface
C_m^*	$= C_\mathrm{m} l/a$
C_s	coefficient accounting for the thermal slip at the particle surface
C_t	coefficient accounting for the temperature jump at the particle surface
C_t^*	$= C_\mathrm{t} l/a$
D_n', D_n''	functions of ρ and z defined by Eqs. (A.6) (m^{-n+1})
d	distance between the particle center and the plane wall (m)
E^2	the Stokes operator defined by Eq. (18) (m^{-2})
$G_n^{-1/2}$	the Gegenbauer polynomial of the first kind of order n and degree $-1/2$
H_n	coefficients in Eq. (11) for the internal temperature field
I	intensity of the incident light beam ($\mathrm{W\,m}^{-2}$)
J	the photophoretic asymmetry factor of the particle defined by Eq. (31)
J_n	the Bessel function of the first kind of order n
k	thermal conductivity of the fluid ($\mathrm{W\ m}^{-1}\mathrm{K}^{-1}$)
k_p	thermal conductivity of the particle ($\mathrm{W\,m}^{-1}\mathrm{K}^{-1}$)
k^*	$= k_\mathrm{p}/k$
l	mean free path of the gas molecules (m)
P_n	the Legendre polynomial of order n
r	radial spherical coordinate (m)
$S_n(\zeta)$	function of ζ defined by Eq. (12)
T	temperature distribution in the fluid phase (K)
T_n	coefficients in Eqs. (10) and (13) for the external temperature field
T_p	temperature distribution inside the particle (K)
T_0	temperature of the bulk gas and the plane wall (K)
U	photophoretic velocity of a particle ($\mathrm{m\,s}^{-1}$)
U_0	photophoretic velocity of an isolated particle ($\mathrm{m\,s}^{-1}$)
v_r, v_θ	components of the fluid velocity in spherical coordinates ($\mathrm{m\,s}^{-1}$)
v_ρ, v_z	components of the fluid velocity in cylindrical coordinates ($\mathrm{m\,s}^{-1}$)
z	axial cylindrical coordinate (m)

Greek letters

α_n', α_n''	functions of ρ and z defined by Eqs. (A.1) (m^{-n-1})
β_n', β_n''	functions of ρ and z defined by Eqs. (A.2) (m^{-n-1})
δ_n', δ_n''	functions of ρ and z defined by Eqs. (A.3) (m^{-n+1})
ζ	$= r/a$
η	viscosity of the fluid ($\mathrm{kg\,m}^{-1}\mathrm{s}^{-1}$)
θ, ϕ	angular spherical coordinates
λ	the wavelength of the incident light beam (m)
υ, κ	real and imaginary parts of the complex refractive index $\overline{N}$ of the particle
ρ	radial cylindrical coordinate (m)
ρ_f	density of the fluid ($\mathrm{kg\,m}^{-3}$)
Ψ	Stokes stream function for the fluid flow ($\mathrm{m}^3\mathrm{s}^{-1}$)

References

[1] C. Orr, E.Y.H. Keng, J. Atmos. Sci. 21 (1964) 475–478.
[2] J.C. Maxwell, Philos. Trans. R. Soc. 170 (1879) 231–256.
[3] E.H. Kennard, Kinetic Theory of Gases, McGraw–Hill, New York, 1938, pp. 291–337.
[4] O. Preining, in: C.N. Davies (Ed.), Aerosol Science, Academic Press, New York, 1966, pp. 111–135.
[5] S. Arnold, M.J. Lewittes, J. Appl. Phys. 53 (1982) 5314–5319.
[6] V. Chernyak, S. Beresnev, J. Aerosol Sci. 24 (1993) 857–866.
[7] M. Kerker, D.D. Cooke, J. Opt. Soc. Am. 72 (1982) 1267–1272.
[8] D.W. Mackowski, Int. J. Heat Mass Transfer 32 (1989) 843–854.
[9] L.D. Reed, J. Aerosol Sci. 8 (1977) 123–131.
[10] Yu.I. Yalamov, V.B. Kutukov, E.R. Shchukin, J. Colloid Interface Sci. 57 (1976) 564–571.
[11] L. Talbot, R.K. Cheng, R.W. Schefer, D.R. Willis, J. Fluid Mech. 101 (1980) 737–758.
[12] C. Cercignani, Rarefied Gas Dynamics: From Basic Concepts to Actual Calculations, Cambridge Univ. Press, Cambridge, UK, 2000.
[13] Y. Sone, Kinetic Theory and Fluid Dynamics, Birkhauser, Boston, 2002.
[14] H.J. Keh, Aerosol Air Quality Res. 1 (2001) 21–30.
[15] W.M. Greene, R.E. Spjut, E. Bar-Ziv, A.F. Sarofim, J.P. Longwell, J. Opt. Soc. Am. B 2 (1985) 998–1004.
[16] A.F.M. Akhtaruzzaman, S.P. Lin, J. Colloid Interface Sci. 61 (1977) 170–182.
[17] V. O'Brien, AIChE J. 14 (1968) 870–875.
[18] M.J. Gluckman, R. Pfeffer, S. Weinbaum, J. Fluid Mech. 50 (1971) 705–740.
[19] P. Ganatos, R. Pfeffer, S. Weinbaum, J. Fluid Mech. 99 (1980) 739–753.
[20] J.R. Brock, J. Colloid Sci. 17 (1962) 768–780.
[21] J. Happel, H. Brenner, Low Reynolds Number Hydrodynamics, Martinus Nijhoff, The Netherlands, 1983.
[22] J.H. Lienhard, A Heat Transfer Textbook, second ed., Prentice-Hall, Englewood Cliffs, NJ, 1987.
[23] H.J. Keh, L.C. Lien, J. Fluid Mech. 224 (1991) 305–333.
[24] S.H. Chen, H.J. Keh, J. Aerosol Sci. 26 (1995) 429–444.
[25] S.H. Chen, H.J. Keh, J. Colloid Interface Sci. 171 (1995) 63–72.
[26] S.A. Beresnev, L.B. Kochneva, Atmos. Oceanic Optics 16 (2003) 119–126.
[27] D.P. Shoemaker, C.W. Garland, J.I. Steinfeld, J.W. Nibler, Experiments in Physical Chemistry, fourth ed., McGraw–Hill, New York, 1981.